THE ASTROPHYSICAL JOURNAL, 545:758–771, 2000 December 20

THE RECENT HIGH STATE OF THE BL LACERTAE OBJECT AO 0235 AND CROSS-CORRELATIONS BETWEEN OPTICAL AND RADIO BANDS

M. ROY,[1,2] I. E. PAPADAKIS,[3] E. RAMOS-COLÓN,[4] R. SAMBRUNA,[5] K. TSINGANOS,[3]
J. PAPAMASTORAKIS,[3] AND M. KAFATOS[1]

Received 2000 April 24; accepted 2000 August 2

ABSTRACT

We present new optical (B, V, R, I) and radio (at 14.5, 8.5, and 4.8 GHz) observations of the γ-ray–loud blazar AO 0235+164 obtained during the high state of 1997 December–1998 January. The data were combined with historical light curves from the literature to study correlated optical and radio variations over a time span of more than 20 years. Flux variability with large and energy-dependent amplitude is observed at both wave bands, with the source varying over all timescales sampled (years-months-days), in agreement with previous reports. We have performed a cross-correlation analysis of optical and radio light curves applying various detailed statistical methods. The principal results of our analysis can be summarized as follows: (1) we find that the optical and radio variations exhibit correlated flux changes at their "average" level, stressing the conclusion that the same emission mechanism is responsible for the radiation in the two bands (i.e., synchrotron emission from shocked plasma in the jet). However, as previously reported, a few strong flares at optical do not have obvious counterparts at longer wavelengths, possibly indicating that an additional component is present in the optical (e.g., microlensing), or, alternatively, rapid cooling of the synchrotron particles in a radiative shock. (2) Periodic variations are observed at radio frequencies (14.5 and 8.0 GHz) with a pattern repeating every $\sim$5.8 years, as indicated by the Lomb-Scargle periodogram. This is the first report for periodicity at radio wavelengths for this source; future continuous monitoring is needed to confirm this result. (3) Through the analysis of $B-V$ and $R-I$ slopes, we observe large spectral variations, with a "bimodal" behavior. In the first state, the emission is consistent with a variable power law all across the sampled optical region (from R to V bands); in the second state, the $R-I$ slope is constant while the $B-V$ slope varies, i.e., the continuum has various degrees of curvature at the shorter wavelengths. In general, the power-law slope is not correlated with the flux of the source. However, there is an indication that when the source is in the first state, the spectrum becomes softer as the source brightens.

Subject headings: BL Lacertae objects: individual (AO 0235+164) — galaxies: active — radio continuum: galaxies

1. INTRODUCTION

The radio source AO 0235+164 identified by Spinrad & Smith (1975) as a BL Lac object, is one of the most exceptional and complex blazars. It shows large-amplitude, rapid variations in all wave bands, from radio to γ-rays. It has been classified as an optically violent variable (OVV) blazar (Burbidge & Hewitt 1992; Schramm et al. 1994) and grouped in radio-selected BL Lac objects (RBLs) and 1 Jy source (Giommi et al. 1990; Stickel et al. 1991; Hewitt & Burbidge 1993; Thompson et al. 1995).

In the radio band, AO 0235+164 exhibits large-amplitude outbursts with variability timescales ranging from years to weeks (O'Dell et al. 1988; Teräsranta et al. 1992; Schramm et al. 1994; Chu et al. 1996; Kraus et al. 1999) and less than a day (Quirrenbach et al. 1992; Romero et al. 1997; Kraus et al. 1999). Observations with VLBI (e.g., Jones et al. 1984; Bååth 1984; Gabuzda & Cawthorne 1996; Chu et al. 1996; Shen et al. 1997) have revealed a very compact radio source. Superluminal motions with extremely high apparent velocities, probably up to $\beta_{\rm app} \simeq 30$, have also been observed (Impey 1987).

In the optical wave bands, the source is characterized by a very steep optical spectrum (Smith et al. 1987; Brown et al. 1989). Long-term monitoring has revealed pronounced, very large amplitude variability characterized by sharp rises and declines (Takalo et al. 1998). Polarization measurements have detected it as a highly polarized source ($\sim$25%) (Rieke et al. 1976; MacLeod et al. 1976; Ledden et al. 1976; Angel & Stockman 1980; Mead et al. 1990; Stickel et al. 1991; Webb et al. 1988; Webb 1992). Rapid and large variations in the polarization of the source (up to 44%) have also been observed.

Apart from the flux variability, AO 0235+164 has also shown evidence of optical spectral variations. Brown et al. (1989) found that the optical spectrum changes its slope, α, between -2.9 and -4.8 with an average value of -3.9. They also found that a simple power law is not a good representation of the $U-V$ energy spectrum due to spectral curvature present in the data. Smith et al. (1987) reached similar conclusions and found that $-4 < \alpha < -2$. Webb & Smith (1989) did not find significant spectral changes during the 1987 outburst. Lately, Takalo et al. (1998) reported a mean α of -2.7, and spectral variations that are correlated

[1] Center for Earth Observing and Space Research, Institute for Computational Sciences and Informatics and Department of Physics, George Mason University, Fairfax, VA 22030; mroy@science.gmu.edu, mkafatos@gmu.edu.
[2] Indian Statistical Institute, Calcutta, India.
[3] Physics Department, University of Crete, 710 03 Heraklion, Crete, Greece; jhep@physics.uoc.gr, tsingan@physics.uoc.gr, papamast@physics.uoc.gr.
[4] Department of Mathematics, CUH Station, University of Puerto Rico-Humacao, Humacao, Puerto Rico 00791; eramos@cuhwww.upr.clu.edu.
[5] Pennsylvania State University, Department of Astronomy and Astrophysics, 525 Davey Lab, University Park, PA 16802; rms@astro.psu.edu.

with the source flux state in the sense that the spectrum becomes flatter when the source brightens.

In the X-rays, flux variability of a factor 2 over a timescale of 3 days is observed in a *ROSAT* exposure (Madejski et al. 1996). The X-ray continuum also exhibits spectral variations with the flux, as inferred from comparison of *ROSAT* and *ASCA* data taken 6 months apart, with a trend of a harder spectrum during the fainter flux state (Madejski et al. 1996), contrary to most BL Lac objects bright at X-rays (e.g., Sambruna et al. 1994) and similar to a few other radio-selected sources (Urry et al. 1996). AO 0235+164 was detected at GeV energies with the *Compton Gamma Ray Observatory* (*CGRO*) EGRET experiment (von Montigny et al. 1995), although only a few pointings were obtained and no constraints on variability at these wavelengths are available (Mukherjee et al. 1997).

AO 0235+164 has been one of the first blazars where correlated radio and optical variability was claimed (Rieke et al. 1976; Balonek & Dent 1980). Clements et al. (1995), based on a cross-correlation analysis between long-term optical and radio light curves, found that the radio variations follow those at the optical band with a delay of about 2 months. Takalo et al. (1998) found that the "base" emission in the optical is correlated quite well to the 22 and 37 GHz radio flux emission, implying that both are due to synchrotron emission from a relativistic jet. Optical spikes with no radio counterparts, even some of the radio flares (Kraus et al. 1999), could be due to another mechanism such as microlensing.

AO 0235+164 lies in a rich environment, with at least ~ 30 objects in the field. The source itself is at a redshift of $z = 0.94$, as indicated by the emission lines in the optical spectrum (Rieke et al. 1976; Cohen et al. 1987; Yanny et al. 1989). In addition, an absorption-line redshift system has been detected at $z = 0.85$ from an intervening galaxy. Both emission and absorption features have also been identified from a third component at $z = 0.524$ (Roberts et al. 1976; Wolfe et al. 1982). Continued studies on the surrounding region of AO 0235+164 have revealed a number of faint galaxies, mostly at a redshift of $z = 0.524$ (Burbidge et al. 1996). Because of the intervening objects, AO 0235+164 has been considered as one of the best candidates among BL Lac objects in which the variability observed is caused by microlensing by stars in the intervening galaxies.

In this paper we present a detailed study of the optical and radio variability of AO 0235+164 using new radio and optical observations supplemented by data from the literature. Using this extensive data set, and an improved cross-correlation technique, we investigate whether there are any correlations between the optical and radio band variations, as well as between the variations seen at different frequencies within each wave band. We study the optical energy spectrum variations and, using data collected during the latest optical/radio outburst of the source, we construct a contemporaneous multifrequency flare energy spectrum which we compare with the preflare and the average energy spectrum distribution of the object. Finally, we searched the historical radio light curves for periodicities, with interesting results.

In §§ 2 and 3 we present and analyze, respectively, the optical and radio data used in this work, the results from the cross-correlation, the results from the period search of the radio light curves, the results from the optical spectral variability analysis, and the contemporaneous flare/preflare energy distribution of the source. Discussion and conclusions are presented in § 4.

2. THE OPTICAL AND RADIO DATA

The optical data used in this paper were obtained in the ways described below. The final optical data set spans the range from 1979 December to 1998 December.

1. Observations at the Skinakas Observatory in Crete, Greece, during 6 nights in 1998 July. The telescope is a 1.3 m, f/7.7 Ritchey-Chrétien. The observations were carried out through standard Johnson B and V filters, using a 1024×1024 Tektronix CCD with a 24 μm pixel size. A log of the observations is presented in Table 1. The exposure time was 300 and 150 s for the B and V filter, respectively (the numbers in parentheses in Table 1 correspond to the UT time of the midpoint of the corresponding exposure). Comparison stars for the AO 0235+164 photometry were taken from McGimsey et al. (1976) and Smith et al. (1985).

2. Historical B, V, R, and I light curves during the period 1979 December (MJD = 44,226.50) and 1998 September (MJD = 51,078.389), kindly provided by A. Sillanpää and L. Takalo, part of which (up to 1996 July) were previously published in Takalo et al. (1998).

3. Data from the public database NED available on the Web, including data taken during the period from 1997 November to 1998 December. These data were obtained by various authors as part of different observing programs.

Since the source has a substantial amount of intervening material because of the presence of the extended faint system at $z = 0.524$, it is important to estimate the extinction and correct the calibrated magnitudes for reddening. Here we assume a galactic type of extinction following Cardelli et al. (1989). In order to estimate the V-band extinction (in magnitudes A_V) we used the following relationship,

$$A_V = \frac{N_{\rm H}}{2.23 \times 10^{21}}$$

(Ryter 1996). Here we assume the column density $N_{\rm H}$ derived from X-ray measurements with *ROSAT* (Madejski et al. 1996): $N_{\rm H} = 4.33 \times 10^{21}$ cm^{-2}, which implies $A_V = 1.94$. This is much higher than the Galactic value from 21 cm measurements, and is most likely due to absorption by neutral metals in the gas in the intervening galaxies (see § 1). Using the A_λ versus λ relationship of Cardelli et al. (1989), we found the extinction (in magnitudes) in the other filters as well: $A_B = 2.60$, $A_R = 1.55$, $A_I = 1.164$.

TABLE 1

SKINAKA'S OBSERVATION LOG

Day (1998 July)	B	V
13	15.84±0.06 (01:51)	14.92±0.04 (01:13)
16	15.80±0.03 (01:42)	14.88±0.01 (01:30)
21	15.89±0.02 (01:15)	14.97±0.01 (01:10)
22	15.97±0.02 (01:21)	15.06±0.01 (01:12)
23	16.02±0.02 (01:12)	15.09±0.02 (01:02)
24	16.07±0.03 (01:18)	15.16±0.02 (01:08)

NOTE.—Numbers in parentheses are comparison stars for the AO 0235+164 photometry were taken from McGimsey et al. (1976) and Smith et al. (1985).

The radio data used here (1975 September–1999 March) are from the University of Michigan Radio Astronomy Observatory (UMRAO), in the form of integrated total flux densities at 4.8, 8.0, and 14.5 GHz, taken as averages over 30 days. Light curves with the data prior to 1995 have already been presented by Aller et al. (1999).

2.1. *The Optical and Radio Historical Light Curves*

Figure 1 shows a plot of the *B*, *V*, *R*, and *I* historical light curves of AO 0235+164. In this figure, we have converted the optical dereddened magnitudes to flux (in mJy). The errors on the flux were estimated using the standard formula for the propagation of errors, e.g., equation (4.8) in Bevington (1969). The source is highly variable on all bands and at all sampled timescales. The labels "op1" (MJD 42,689.50–42,750.50 $\approx$ first week, 1975 October–last week, 1975 December), "op2" (MJD 43,901.50–43,914.50 $\approx$ last week, 1979 January–first week, 1979 February) and "op3" (MJD 46,793.50–46,824.50 $\approx$ last week, 1986 December–last week, 1987 January) indicate the previously known large-amplitude outbursts (O'Dell et al. 1977; Pica et al. 1980; Webb & Smith 1989, respectively). After "op3," the next outburst was observed in early 1990 ("op4" in Fig. 1, MJD 47,893.50–48,269.50 $\approx$ last week, 1989 December–mid 1991 January) and then the source gradually faded until early 1996, when the faintest ever optical source level was recorded (Takalo et al. 1998). The source started to increase its flux again in 1997 when it began a $\sim$2.5 mag outburst in 1997 December ($\approx$MJD 50,792.5). When observations resumed in 1998 July (MJD $\approx$ 51,018.50) the source was at an even brighter state. Apparently, after late 1997 the source entered into a new, rather long "flaring" state which lasted until 1998 December ($\approx$MJD 51,200.50), when the present data set stops.

The individual light curves in Figure 1 have a different observational sampling, therefore not all outbursts can be identified in each one of them. In all cases when the data sampling is similar, the variability pattern is similar as well (e.g., the *V* and *R* light curves between MJD $\sim$49,000 to $\sim$51,000, and all the light curves around the "op4" peak). The maximum variation, Δmag, in the light curves is $\Delta\mathrm{mag}_B \sim 6$, $\Delta\mathrm{mag}_V \sim 6.5$, $\Delta\mathrm{mag}_V \sim 5.5$, and $\Delta\mathrm{mag}_I \sim 4.5$.

Figure 2 shows a plot of the radio band historical light curves (i.e., 14.5 , 8.0 , and 4.8 GHz). As with the *B*-band light curve, we have labeled the most significant peaks in the 14.5 GHz light curve ("rp1," "rp2," "rp3," "rp4," and "rp5"). In general, when compared to the optical, the radio light curves show smoother variations and are less erratic. However, the scarcity of data, mainly in the optical band, makes difficult a detailed comparison. The optical flares "op1," "op3," and "op5" correspond to the radio flares "rp1," "rp3," and "rp5." There is a moderate radio outburst during the "op4" flare, but we have noted with "rp4" the following large radio flare (MJD 48,850.50–49,064.50 $\approx$ 1992 August, 15–1993 March, 16), during which we have no optical data. The same is true for the "rp2" flare (MJD 45,018.50–45,073.50 $\approx$ second week, 1982 February–second week, 1982 April), which does not correspond to an optical one, probably because of limited optical data coverage. On the other hand, "op2," one of the largest amplitude and best-sampled outbursts in the *B* band, does not correspond to a similar radio outburst. A similar radio flare could not

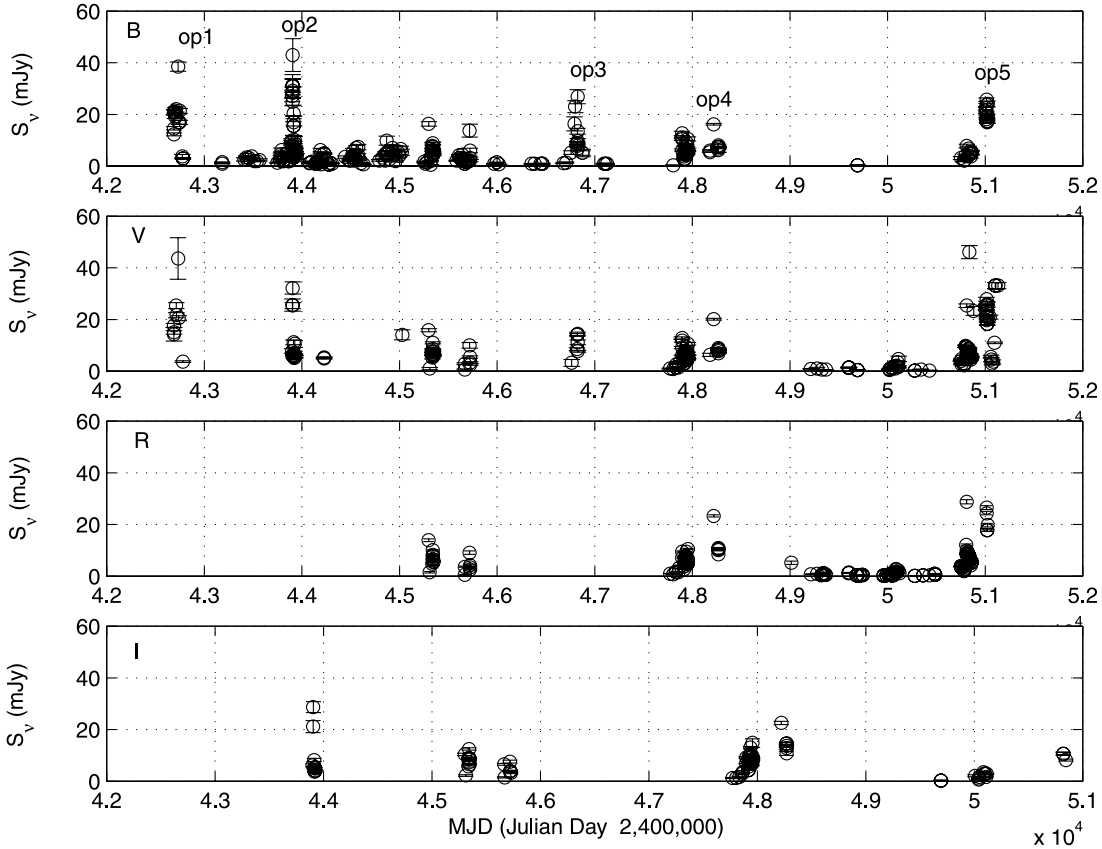

FIG. 1.—Historical *B*-, *V*-, *R*-, and *I*-band light curves of AO 0235+164. The numbers following the label "op" indicate the major optical outbursts since 1975.

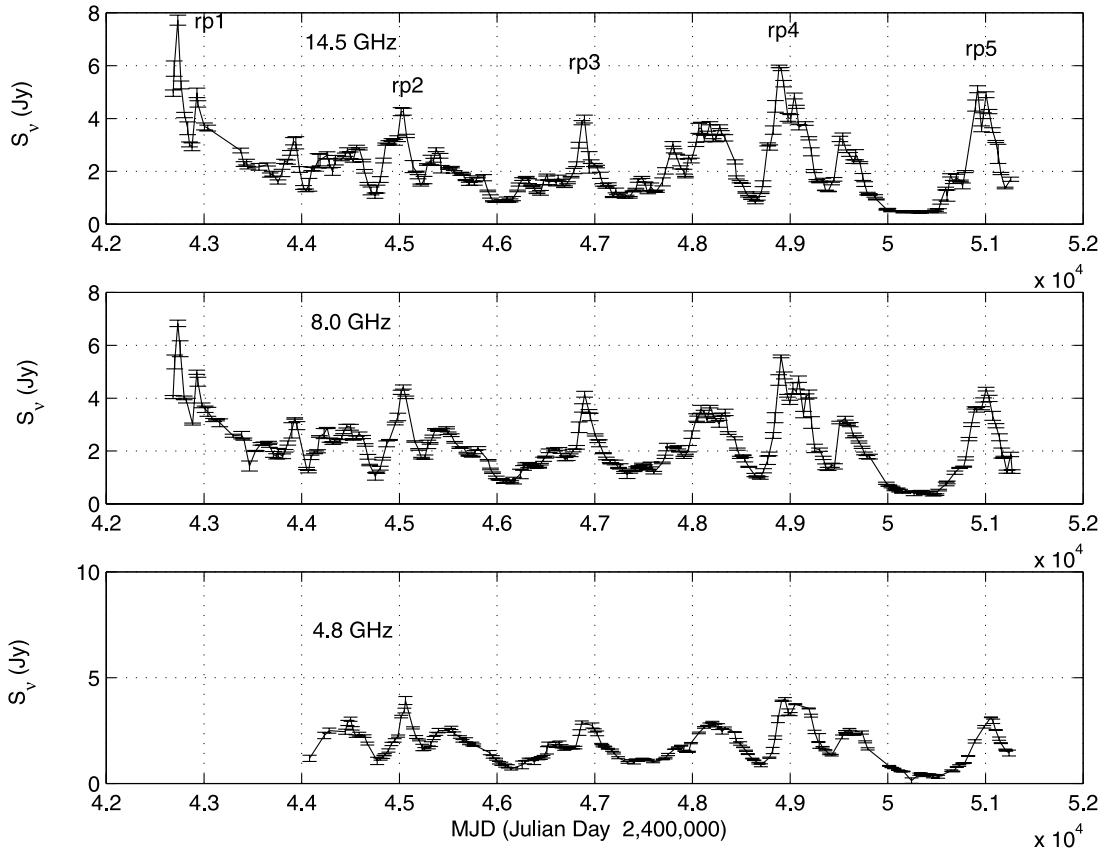

FIG. 2.—Historical radio-band light curves in 4.8, 8.0, and 14.5 GHz of AO 0235+164. The numbers following the label "rp" indicate the major radio outbursts since 1975.

be missed, since the time coverage in the radio bands is much better than in the optical.

Within the radio band, the light curves at the three different frequencies show a similar variability behavior. The flares identified in the 14.5 GHz light curve can also be seen in the other two light curves. The main difference is that the amplitude is smaller in the 8.0 GHz and decreases even further in the 4.8 GHz light curve. In order to quantify this difference we estimated the "normalized variability amplitude,"

$$A = \sigma_{\rm source}/\hat{x} \ ,$$

where $\hat{x}$ is the mean of the light curve, and $\sigma_{\rm source}$ is the source standard deviation,

$$\sigma_{\rm source} = \sqrt{\sum_i (x_i - \hat{x})^2/N - \sigma^2_{\rm noise}} \ ,$$

with $\sigma^2_{\rm noise} = \sum_i {\rm err}(i)^2/N$ [err(i) is the error of each point]. We found that $A_{14.5\rm GHz} = 55\%$, $A_{8.0\rm GHz} = 49\%$, and $A_{4.8\rm GHz} = 45\%$.

We also calculated the variability amplitudes for the optical band light curves: $A_B = 113\%$, $A_V = 87\%$, $A_R = 77\%$, and $A_I = 65\%$. As expected, the variability amplitudes are larger in the optical than in the radio band light curves. Interestingly, the large values for the B- and V-band light curves imply that $\sigma \sim \hat{x}$ in these cases. This result suggests that the optical light curves of AO 0235+164 are either nonlinear or non-Gaussian (Leighly 1999).

2.2. *The Recent (Late 1997–1998) Outburst*

Figure 3 shows a plot of the B, V, and R light curves after MJD 50,700 (~early 1997 September). For clarity reasons, in this figure we have shifted the B and R light curves (B divided by 1.6 and R multiplied by 1.4). On 1997 December 1 (MJD 50,791.50) the source begun an outburst which saw it brighter than $V < 13$ and $R < 12.5$ ("op6" in Fig. 3). These are among the brightest values recorded for this object in those bands. The source faded and then brightened again on 1998 January 16 (MJD 50,819.50, "op7" in the same figure; this flare is best sampled in the V-band light curve). This "double peak" morphology resembles that of the previous reported outbursts (Webb & Smith 1989). However, the behavior of the source after this burst was different from that of the previous one. One V point on 1998 March 3 (MJD 50,877.50) showed that the source did not return to its "base" level. In fact, in 1998 July, the source was still in a very high state ("op8," MJD 51,007–51, 023 = 1998 July 13–29). After late 1998 August, the source decreased its V-band flux by ~2 mag within 20 days, but then immediately started to brighten again until the end of 1998. In fact, our last V measurement (1998 December, MJD = 51,159.50) is $V = 11.66$, which is one of the highest values recorded for this object in this band.

The optical light curves during the 1997 December–1998 December period look quite similar. Although the data sampling is not the same, the "op6" and "op7" flares appear to have a similar amplitude and happen approx-

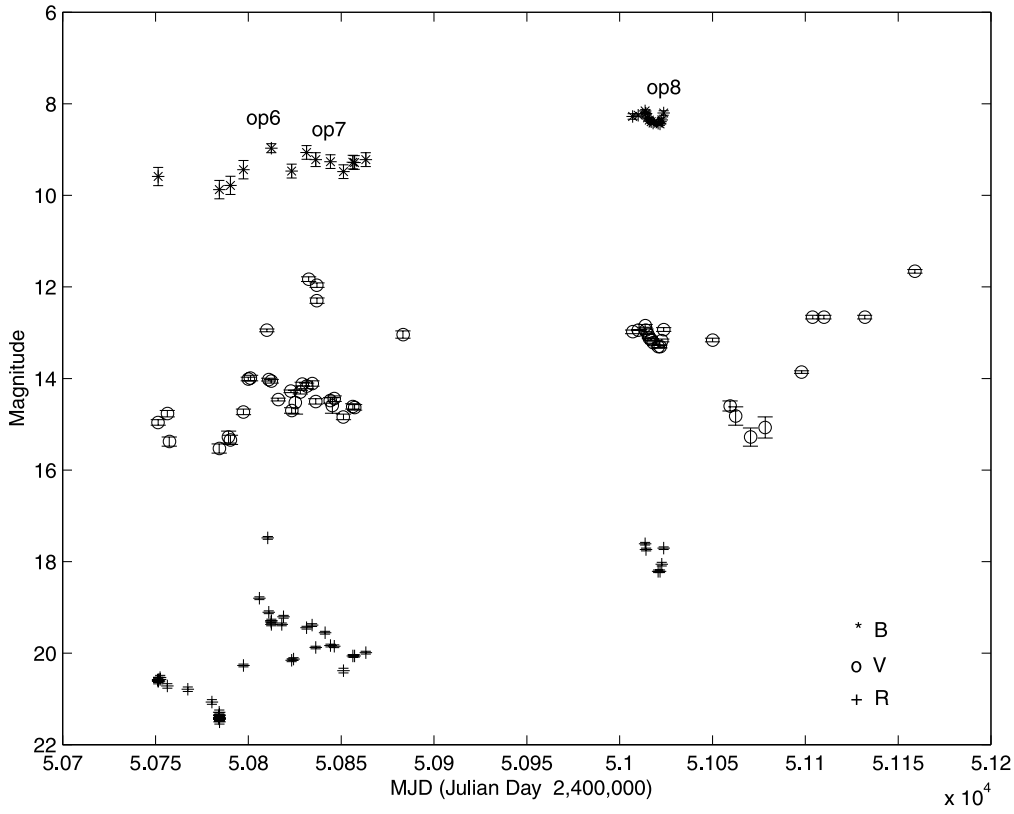

FIG. 3.—*B*-, *V*-, and *R*-band light curves of AO 0235+164 during the recent flaring state (1997 September–1998 December) with *B* magnitudes divided by 1.6 and that of *R* multiplied by 1.2. The numbers after the label "op" indicate individual flares in the light curves.

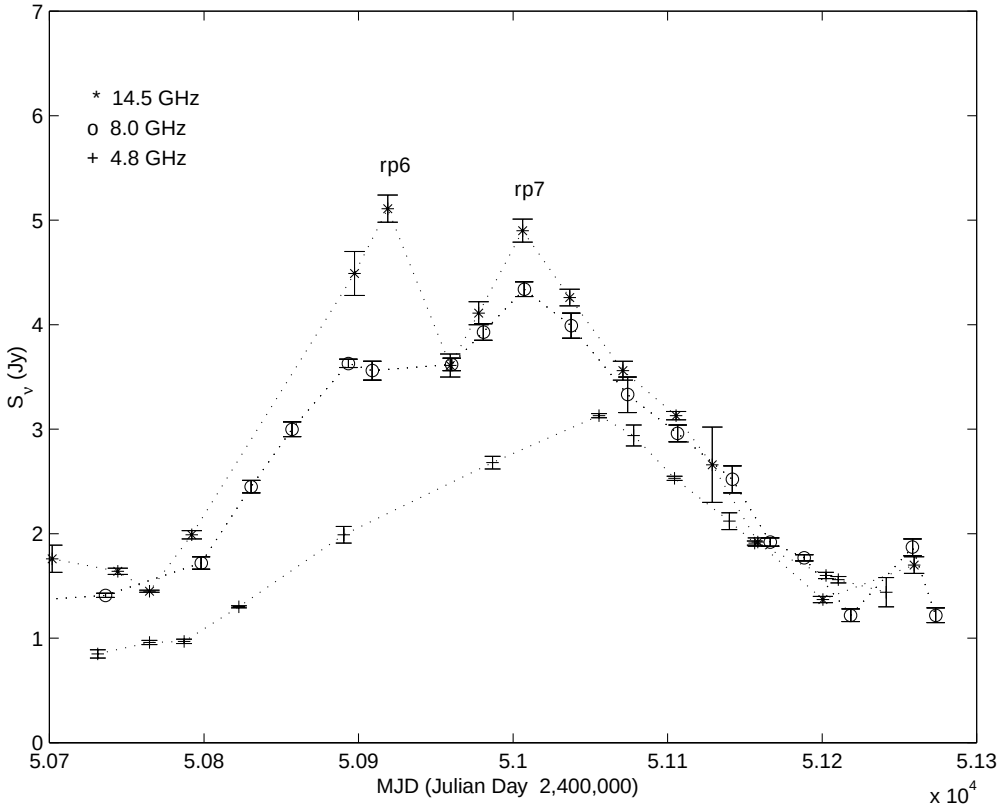

FIG. 4.—4.8, 8.0, and 14.5 GHz light curves of AO 0235+164 during the same period as in Fig. 3. The numbers after the label "rp" indicate individual flares in the radio light curves.

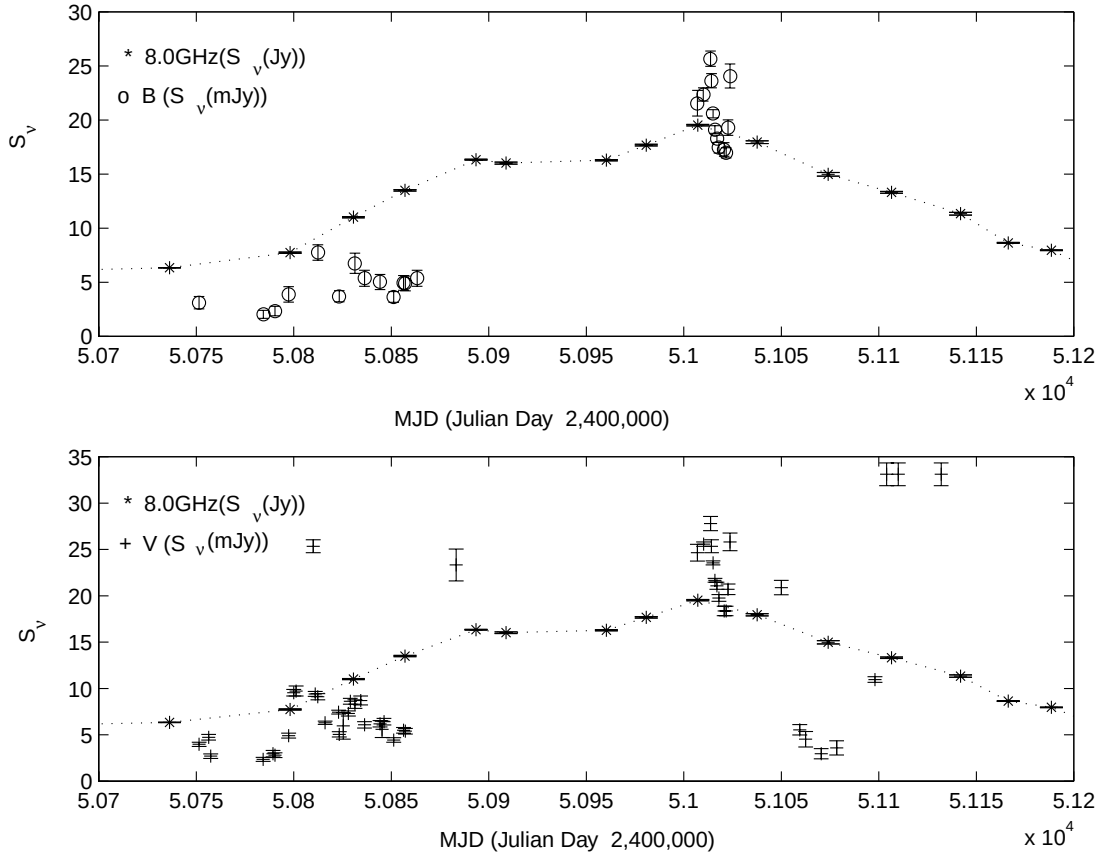

FIG. 5.—Plot of the *B*- and *V*-band light curves together with the 8.0 GHz band light curve (*upper and lower panels*, respectively) during the recent flaring period of AO 0235+164 (late 1997/1998). In this figure, we have plotted the optical band light curves after converting the dereddened magnitudes to flux. For clarity, the 8.0 GHz light curve has been multiplied by a factor of 4.5.

imately simultaneously in all bands. The "op8" peaks appear stronger than "op6" in the *B* and *R* bands, but this is probably due to the fact that we have not sampled the maximum amplitude of "op6" in these bands (mainly *B*).

Figure 4 shows the radio light curves during the same "flaring" period. The source started increasing its radio flux in 1997 December until early April, when it reached its maximum in the 14.5 GHz band. It stayed at a high flux level exhibiting a double-peak morphology until 1998, mid-July ("rp6," MJD 50,918.5 ≈ 1998, 14th April, and "rp7," MJD 51,006.5 ≈ 1998, July 10, in Fig. 4). Then it started fading in all three bands, returning to its "base" flux level by 1999 January. The three radio light curves show the same "global" behavior with each other but there also exist some differences. For example, "rp7" has a smaller amplitude in the 8.0 GHz band, and is missing in the 4.8 GHz light curve (perhaps this is due to the sampling pattern of this light curve).

Figure 5 shows the *B*- and *V*-band light curves plotted together with the 8.0 GHz light curve during the late 1997 and 1998 flaring phase of AO 0235+164 (the 8.0 GHz flux values are multiplied by 4.5 for clarity). Although both the radio and optical light curves have extended gaps in them, some trends can be recognized. On the average the variability behavior in these two frequency regimes is similar. For example, between MJD 50,750 and MJD 50,900, the source brightens in the optical and radio; it stays bright for ∼100–150 days and then starts to fade in both of them. However, apart from this broad similarity, the optical light curves are far more erratic than the radio. The 1997 December optical outburst does not show a simultaneous radio counterpart (one is tempted to identify the "rp6" and "rp7" radio peaks as the delayed response of the the optical flares "op6" and "op7" in the radio band), the decline after 1998 August is much faster in the *V*-band, and the fast, very large amplitude flux increase in the same band toward the end of 1998 is totally missing in the radio light curve.

3. DATA ANALYSIS

3.1. *Correlation Study of Multiwavelength Time Series*

In order to investigate whether the optical and radio variability of the source are related, we computed cross-correlation functions between different band light curves. Cross-correlation function (CCF) analysis is a standard technique in time series analysis. The CCF measures the amount of similarity or correlation between two time series (i.e., light curves) as a function of the time shift between them. It is formally defined as

$$\mathrm{CCF}(\tau) = \frac{E[a(t) - E_a][b(t+\tau) - E_b]}{\sqrt{V_a V_b}}, \qquad (1)$$

where $a(t)$ and $b(t)$ are two light curves, τ is the time lag, E the expectation value, and V the variance over the light curves. The lag (τ) corresponding to the peak in the CCF is interpreted as a quantifier of the delay between two time series.

The definition of the CCF assumes that the sampling in the light curves is uniform. However, in most cases the sampling is not uniform. In general, approximation schemes have to be employed in order to estimate the delay from equation (1). The most common approximation technique is the interpolated cross-correlation function (ICCF) method of Gaskell & Peterson (1987) that uses a linear interpolation scheme to determine the missing data in the light curve. The most common approximation technique is the interpolated cross-correlation function (ICCF) method of Gaskell & Peterson (1987), which uses a linear interpolation scheme to determine the missing data in the light curve. In this way the cross-correlation is performed twice, interpolating first in one time series and then in the other, and taking the average of the results. For the case of interpolation in time series b the cross-correlation function is approximated by

$$\mathrm{ICCF}(\tau) = \frac{1}{N} \sum \frac{(a_i - \bar{a})\{L[b(t+\tau)] - \bar{b}\}}{\sigma_a \sigma_b}, \qquad (2)$$

where L indicates a piecewise linear interpolation of series b at time $t + \tau$ and N is the number of data points in a. The ICCF works reasonably well under the assumption that the variations in the light curve are smooth.

On the other hand, the discrete correlation function (DCF) (Edelson & Krolik 1988) utilizes a binning scheme to approximate the missing data. The cross-correlation function is estimated by

$$\mathrm{DCF}(\tau) = \frac{1}{M} \sum \frac{(a_i - \bar{a})(b_j - \bar{b})}{\sigma_a \sigma_b}, \qquad (3)$$

where the summation is over the M pairs for which $\tau - \Delta\tau/2 \le t_j - t_i < \tau + \Delta\tau/2$. Note that in functions (2) and (3) σ_a and σ_b are the standard deviations for the *entire* light curves.

The errors in the DCF are estimated from the standard deviation in each bin. Both methods are the most commonly applied in the literature but they pose several limitations. The DCF does not give reasonable results if the number of data points is limited. Moreover, both methods are unable to provide estimates of the uncertainties in the estimated lags. The only way to estimate uncertainties is by using assumption-dependent Monte Carlo simulations.

Apart from the ICCF and DCF, there is one more method of estimating the CCF in the case of nonuniformly sampled light curves, namely, the z-transformed discrete correlation function formulation (ZDCF; Alexander 1997). The ZDCF, like the DCF technique, is a binning type of method and can be considered as an improvement of the DCF technique. The ZDCF scheme is based in the calculation of the cross-correlation function CCF(τ) from the correlation coefficient between two time series:

$$r = \sum_i^n \frac{(a_i - \bar{a})(b_i - \bar{b})/(n+1)}{s_a s_b}, \qquad (4)$$

where n is the number of time series pairs in a given time-lag bin and, unlike the DCF formulation, the standard deviations s_a and s_b are used to normalize each individual bin. This definition is particularly important for the case of nonstationary light curves since the summation only considers those points that actually contribute to the bin. The calculation of r is characterized by the highly skewed and nonnormal nature of the sampling distribution, which results in inaccurate estimates of the sample variance. The ZDCF technique circumvents this difficulty by applying Fisher's z-transform of r:

$$z = \frac{1}{2} \log\left(\frac{1+r}{1-r}\right), \quad r = \tanh z, \qquad (5)$$

in order to obtain an approximately normal distribution from which the error intervals in r can be calculated. The calculation of the ZDCF is then

$$r_{\mathrm{dcf}}(\tau) = r^{+[\tanh(\bar{z}+s_z)-r]}_{-[r-\tanh(\bar{z}-s_z)]}, \qquad (6)$$

where $\bar{z}$ and s_z^2 are the mean and variance of z. The validity of these assumptions have been tested with numerical simulations and in practice have shown that the calculation of the ZDCF is more robust than the ICF and the DCF methods when applied to very sparsely and irregularly sampled light curves (see, e.g., Edelson et al. 1996; Giveon 1999). Another notable feature of the ZDCF method is that the data are binned by equal population rather than into bins of equal width $\Delta\tau$. Finally, the ZDCF method estimates the peak in the ZDCF profile using a maximum likelihood function that can be used to estimate the uncertainties in the lags (Alexander 1997).

We used the ICCF and the ZDCF techniques to estimate the CCF between the light curves within the radio band, and between the light curves within optical and radio regimes (for the optical data we used the flux-converted, dereddened magnitude light curves). Because of their inadequate temporal coverage, we could not estimate a reliable cross-correlation function between light curves within the optical regime. Although the data sampling of the B-band light curve is reasonably good until $\sim$1990 (Fig. 1), the other light curves (mainly V and R) are not equally well sampled. In fact the sampling in these light curves improves after $\sim$1990, contrary to what happens in the B band.

Both the ICCF and ZDCF techniques produced similar results for the correlation between the well-sampled radio light curves. Figure 6 shows a plot of the 14.5 GHz versus the 4.8 GHz cross-correlation function, estimated with the ICCF technique for delays in the range between -1000 and 1000 days computing the values of the correlation function

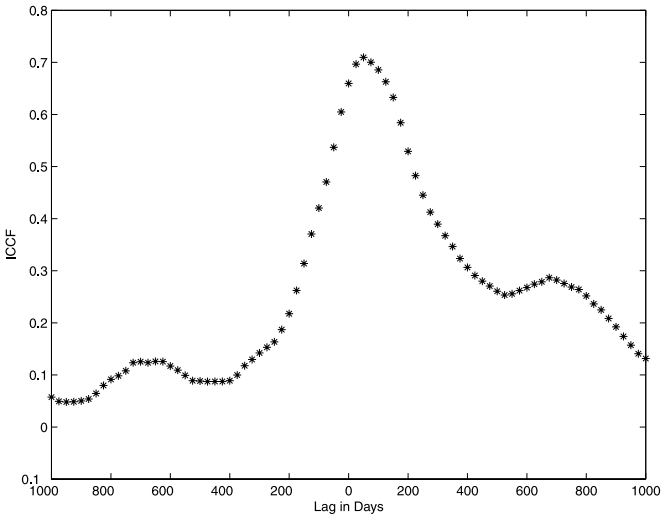

FIG. 6.—Cross-correlation function for the 14.5 GHz vs. the 4.8 GHz light curve. The CCF was estimated using the ICCF method. The maximum r-value is at lag = 50 days, indicating that the 14.5 GHz variations lead those in the 4.8 GHz light curve.

in steps of 25 days. The maximum correlation coefficient is at lag = 50 days. The positive lag in this case shows that the 14.5 GHz variations are leading those in the 4.8 GHz light curve.

The results of the ZDCF method when applied to the radio band light curves are listed in Table 2. Column (3) in this table lists the lag values where the maximum positive correlation appears, while in column (4) the correlation coefficient values at these lags, r, are listed. The errors quoted on the lag values represent the 68% confidence regions. The only significant positive correlation is that between the 14.5 and 4.8 GHz light curves. This is reasonable, as these two light curves have the largest frequency separation in the radio band. However, the value $r = 0.62$ shows that the correlation between the 14.5 and 4.8 GHz light curves is not very strong. This result is consistent with the visual inspection of the radio light curves, which shows that the variations in the 4.8 GHz are smoother and of lower amplitude than those in the 14.5 GHz light curve (see discussion in §§ 2.1 and 2.2 and Fig. 4).

In the same table we also list the results from the ZDCF analysis between the B-band light curve (the best-sampled optical light curve) and the radio band light curves. Figure 7 shows the profile of the ZDCF calculation for the B filter and the 14.5 GHz light curves (the binning of the ZDCF is described in Alexander 1997). All measured CCFs between the B-band and radio band light curves show positive lag values (Table 2), indicating that the optical variations lead those in the radio. Because of the strongly uneven sampling of the B light curve, the errors on the lags are large, except the one between the B and 8 GHz light curves, which shows that the optical lead the radio variations by ~3 months. The correlation coefficient values in all cases are smaller than 0.6, indicating as before that the optical/radio correlation is not very strong. This result is in agreement with our discussion in § 2.1 based on visual inspection of the radio and optical light curves (see also Fig. 5).

TABLE 2

RESULTS OF CROSS-CORRELATION (ZDCF)

First Light Curve (1)	Second Light Curve (GHz) (2)	τ (days) (3)	r (4)
14.5 GHz	8.0	$-70.2^{+143.0}_{-24.0}$	0.61
14.5 GHz	4.8	$134.0^{+15.0}_{-113.0}$	0.62
8.0 GHz.....	4.8	$111.0^{+19.0}_{-134.0}$	0.57
B (optical).....	14.5	$42.7^{+16.0}_{-82.0}$	0.62
B (optical).....	8.0	$103.0^{+93.0}_{-19.0}$	0.49
B (optical).....	4.8	$130.0^{+56.0}_{-149.0}$	0.24

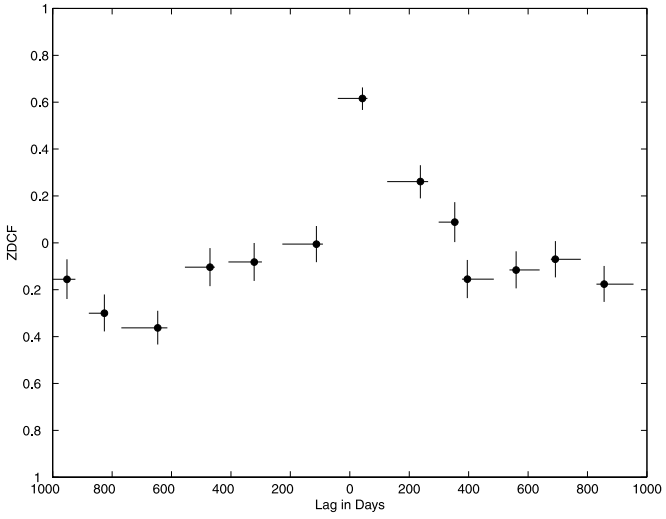

FIG. 7.—Cross-correlation function for the B-band optical light curve vs. the 14.5 GHz light curve. The CCF was estimated using the ZDCF method. A peak of $r = 0.62$ at lag $\tau = 42.7^{+16}_{-82}$ days (see Table 2) is present. The less than 1 value of r indicates that the optical light curve is only moderately well correlated with the radio continuum.

3.2. *Possible Periodicity in the Radio Light Curves of AO 0235+164*

The 14.5 and 8 GHz light curves cover a period of ~24 years (Fig. 2). They show several outbursts with the largest of them ("rp1," "rp2," "rp3," "rp4," and "rp5") separated by a rather constant period of ~2000 days; the last one is the recent 1997/1998 outburst. These outbursts are not sinusoidal, and at least "rp4" and "rp5" show a double-peaked shape.

The regularity in the appearance of the major radio flares motivated us to search for the existence of periodicities in the radio light curves. We used a program based on the Lomb-Scargle periodogram (Lomb 1976; Scargle 1982; the code was taken from Press et al. 1992), to calculate the periodogram of the 14.5 and 8.0 GHz light curves at equispaced frequencies (the 4.8 GHz light curve covers a smaller time period, and the "rp1" flare is missing). The lowest period was the span of the input data, $T = \max(t) - \min(t) = 8405$ days. Higher frequencies were integer multiples of $1/T \sim 0.00012\ \mathrm{day}^{-1}$, and the highest frequency that we examined was $N/(2T) \sim 0.015\ \mathrm{day}^{-1}$.

Figure 8 shows a plot of the low-frequency periodogram of the 14.5 and 8.0 GHz light curves. The dashed horizontal line shows the 10^{-3} significance level, i.e., the probability that one of all the periodogram values will be larger than this level is less than 10^{-3} (this level was calculated under the hypothesis that the variations seen in the light curve are due to Poisson statistics). There are a few peaks above the dashed line in both periodograms. The most significant in

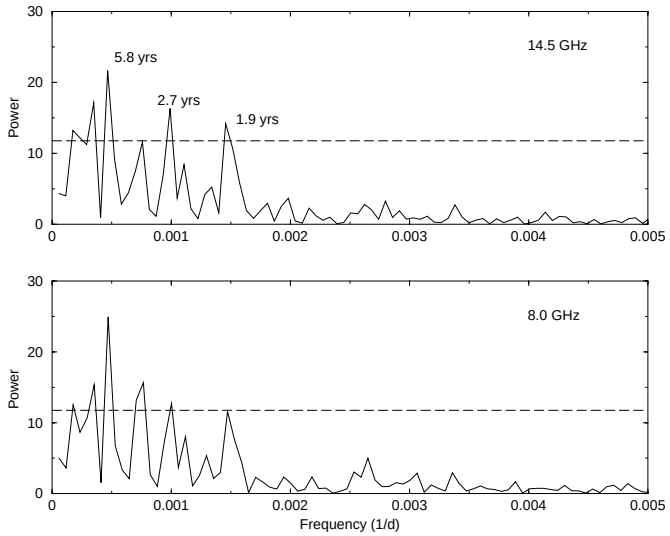

FIG. 8.—Periodogram plots of the 14.5 and 8.0 GHz light curves (*upper and lower panels*, respectively). The long-dashed line in both plots shows the 10^{-3} significance level, under the hypothesis that the variations in the light curves are dominated by Poisson statistics.

both plots corresponds to a period of 5.8 yr, similar to the recurrence period of the significant radio peaks in Figure 2. The two peaks at period 2.7 and 1.9 yr correspond to the first and second harmonics of the main peak. The other significant peaks in the periodograms correspond to a period of 15.65, 7.83, and 3.61 yr. Their existence is not surprising, since, apart from the major outbursts, variations on different timescales are clearly evident in Figure 2.

All the major radio outbursts in Figure 2 (with the possible exception of "rp2") correspond to large-amplitude optical flares. Therefore, we should expect to see evidence of the same periodicity in the optical light curves as well. We estimated the periodogram of the historical B light curve but the results are not conclusive. This is probably because of the strongly uneven sampling of the light curve and the fact that the major optical flares are superimposed on other, smaller amplitude flares that appear to happen at many different timescales (Fig. 1). This combination makes the detection of a similar periodic component in the optical light curves very difficult.

We conclude that, based on the existing radio light curves, there are major outbursts which have a recurrence period of ~ 5.8 yr. The last one occurred in 1998. If this periodicity is a stable characteristic of the source, we should expect the next major radio outburst to occur in late 2003.

3.3. *Optical Spectral Variability*

In order to investigate whether the large-amplitude flux variations in the optical band are associated with spectral variations as well, we used the flux measurements to calculate the two-point spectral indices ($B-V$, α_{BV}, and $R-I$, α_{RI}) using the equation

$$\alpha_{12} = \log (F_1/F_2)/\log (\nu_1/\nu_2) ,$$

where F_1 and F_2 are the flux densities at frequencies ν_1 and ν_2, respectively. The spectral indices were calculated only in those cases in which we have simultaneous B, V and R, I measurements.

Figure 9 shows a plot of α_{BV} versus the $(B+V)$ flux and of α_{RI} versus the $(R+I)$ flux. Both plots show significant variations. The mean slope values are $\bar{\alpha}_{BV} = -0.49 \pm 0.03$ and $\bar{\alpha}_{RI} = -0.98 \pm 0.03$. The χ^2 value for a constant slope 213 with 86 degrees of freedom and 851 with 54 degrees of freedom for the α_{BV} and α_{RI} plots, respectively. The α_{BV} and α_{RI} maximum and minimum values are $\sim(2, -2)$ and $\sim (1, -2)$, respectively.

The plots show clearly that the slope changes are not correlated with the source flux. When we fitted the data in Figure 9 with a straight line, $\alpha = c + s(\text{flux})$, the best-fit value of s is consistent with zero in the case of the α_{BV} plot, $s_{BV} = -0.0004 \pm 0.001$. On the other hand, there appears to be a significant, but very weak, correlation between α_{RI} and source flux: $s_{RI} = 0.02 \pm 0.002$. This value implies that the spectrum becomes flatter (i.e., α_{RI} increases) as the source becomes brighter. We emphasize that this correlation is very weak (the best-fit value of s, although significantly different from zero, is very small) and that it is mainly driven by the few points at large flux states. More simultaneous R and I measurements are needed to confirm the reality of this correlation.

The mean slope values are different, confirming the earlier results on the presence of curvature in the optical spectrum of the source. However, those values are significantly flatter than the previous slope estimates. This difference is due to the different A_V value that we are using. Most of the work that has been done so far on AO 0235+164 was without correcting for extinction or assuming a very small A_V. For example Smith et al. (1987) used $A_V = 0.26$ and found $\bar{\alpha} = -3 \pm 0.4$. Had they used $A_V = 1.96$ their mean slope would be $\bar{\alpha}_{1.96} = \bar{\alpha}_{0.26} + 2.37 = -0.63 \pm 0.4$., i.e., similar to our values.

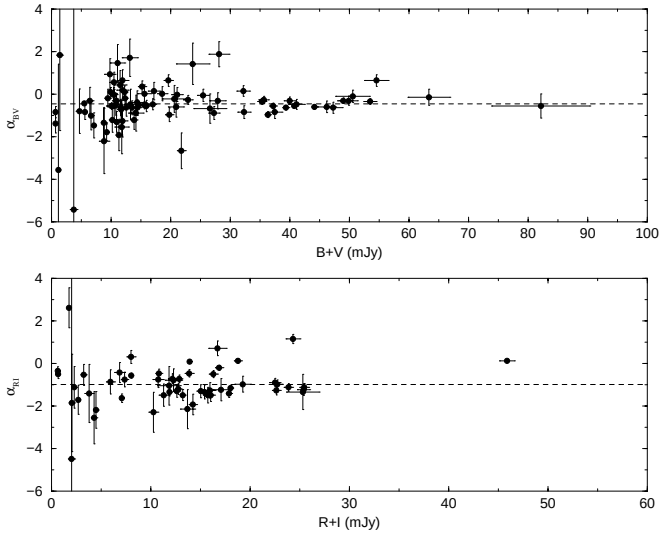

FIG. 9.—Plot of the $B-V$ spectral index vs. the $B+V$ source flux (*upper panel*) and of the $R-I$ index versus the $R+I$ source flux (*lower panel*). In both plots, the slope values are those for which we have simultaneous two-band measurements.

Figure 10 shows a plot of α_{RI} versus α_{BV} for those cases in which we have simultaneous B, V, R, and I observations. In this figure, the dotted line is a plot of the $\alpha_{RI} = \alpha_{BV}$ line. Some points in the plot are consistent with this line. In those cases, the whole B to I spectrum is consistent with a single power law. However, there are also other points not consistent with $\alpha_{RI} = \alpha_{BV}$. Most of them are located to the right of the dotted line, with $\alpha_{RI} \sim -1.3$ and $-1.5 < \alpha_{BV} < 1.5$. It appears that the source can be in two different "spectral states." In the first one, the whole optical

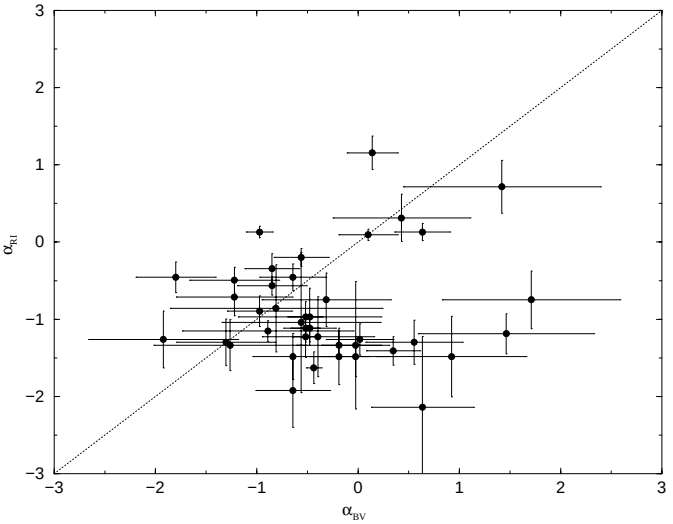

FIG. 10.—Plot of the $B-V$ vs. the $R-I$spectral index values, for those cases in which we have simultaneous B, V, R, and I measurements. The dotted line represents the $\alpha_{BV} = \alpha_{RI}$ line.

spectrum is consistent with a single power law. The slope of the spectrum is variable but not correlated with the source flux. In the second "state," α_{RI} is typically ~ -1.3, but α_{BV} can have any value between ~ -1.5 and ~ 1.5.

Unfortunately, there are only 21 data points for which $\alpha_{BV} \sim a_{RI}$ (first spectral state), and 23 points when $\alpha_{RI} \sim -1.3$ and $-1.5 < \alpha_{BV} < 1.5$ (second state). Therefore, it is not clear whether the two states are related to particular intensity states, i.e., whether they are associated with individual flares. Nevertheless, we investigated whether the power-law slope correlates with the source flux when the source is in the first state. For this reason, we again fitted the α_{BV} versus $(B+V)$ flux with a line, keeping only those points for which $\alpha_{BV} \sim a_{RI}$. The fit is not very good ($\chi^2 = 36.57/20$ dof); however, the best-fit slope value, $s = 0.07 \pm 0.02$, is significantly (i.e., at the $\sim 3\,\sigma$ level) different from zero. This suggests that, when the optical spectrum is well fitted by a single power law as a whole, it becomes softer when the source brightens. More simultaneous, B to I observations are needed in order to investigate further the complex optical spectral variability behavior of this source.

3.4. *Contemporaneous Multifrequency Spectra*

In order to study the spectral evolution of the source, we constructed multiwavelength spectral energy distributions (SEDs) of AO 0235+164 from radio to γ-rays during a low and a high state, using observations as simultaneous/contemporaneous as possible. In particular, AO 0235+164 was observed by *CGRO* EGRET as a Target of Opportunity during 1997 November 3–11. The source was only marginally (1.4 σ) detected, with an upper limit to the integrated flux above 100 MeV of $F(>100\ \mathrm{MeV}) \leq 1.4 \times 10^{-7}$ photons cm^{-2} s^{-1} at 95% confidence. At the time of the γ-ray observation the flux at the longer wavelengths had already faded and the source was in a lower state. We collected radio through optical data as close as possible to the date of the EGRET observation, or November 30 (MJD 50,782.5). Data were also collected during the December flare (December 31, MJD 50,813.5), to characterize the source SED during the high state.

Figure 11 shows the SEDs of AO 0235+164 during the preflare state of November 30 (*filled circles*) and the flare state of December 31 (*crosses*). The open circles represent the "average" SED from nonsimultaneous data at radio through X-rays from Fossati et al. (1998) and Sambruna et al. (1996), and at γ-rays (von Montigny et al. 1995; Hartman et al. 1999). At the high redshift of AO 0235+164 ($z = 0.94$), the K-correction is important; we K-corrected all the fluxes in Figure 11, following the prescription given in Fossati et al. (1998), for consistency. Although the data in Figure 11 are rather scanty and do not sample the SED well, they represent our best possible attempt at contemporaneous (± 3 days) SEDs of the source during a low and high state during the period of our observations.

It is well known that the spectral energy distributions of blazars are typically double-humped. The first component peaks anywhere from IR/optical in the so-called low-energy peaked blazars (LBLs) to UV/X-rays in their higher energy counterparts (high-energy peaked blazars, or HBLs). The rapid flux variability and high polarization of this component leave little doubt that its origin is synchrotron emission from the relativistic electrons in the jet (e.g., Ulrich et al. 1997). The second spectral component extends from X-rays to γ-rays, and its origin is less well understood. A popular emission mechanism is inverse Compton scattering of ambient photons off the jet's electrons (e.g., see the review by Sikora 1994).

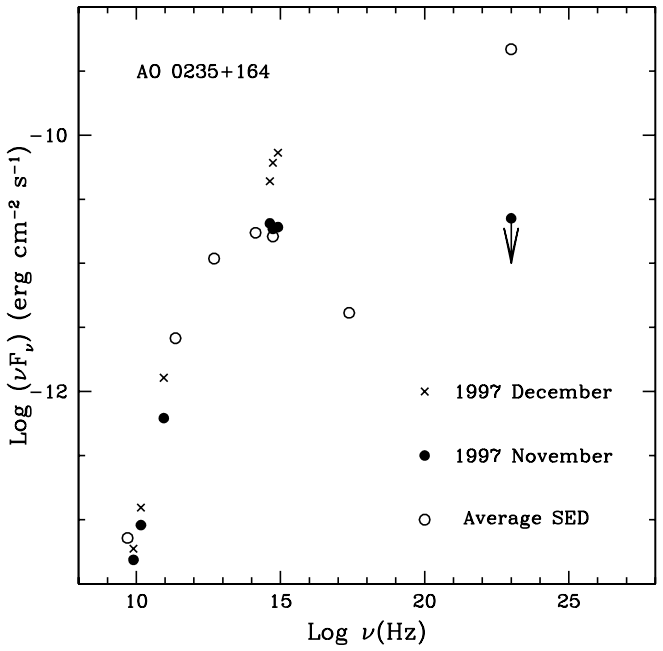

FIG. 11.—Contemporaneous multiwavelength spectral energy distributions (SEDs) of AO 0235+164 during 1997 November (*filled circles*) and 1997 December (*crosses*), for the frequencies considered. The 1997 SEDs are compared to the average SED from nonsimultaneous literature data (Fossati et al. 1998). During the outburst of 1997 December, the source underwent a large increase of flux at all observed wavelengths.

In AO 0235+164, the peak of the synchrotron component in the SED is usually located at IR/optical wavelengths, clearly qualifying this object as an LBL (Sambruna et al. 1996; Giommi et al. 1995). Despite the limited data coverage, it is apparent from Figure 11 that during the preflare state of 1997 November the source was in a "typical" average state. However, during the December outburst, when the flux increased at all wavelengths from radio to optical, the data in Figure 11 suggest that the synchrotron peak was at higher energies than during the quiescent state. More data are needed to confirm this impression; however, if true, the shift of the synchrotron peak in AO 0235+164 would be similar to what was observed in the HBL Mrk 501, where the synchrotron peak frequencies were observed to move from 10^{15}–10^{16} Hz to $\geq 10^{19}$ Hz during a period of intense correlated TeV and X-ray activity (Pian et al. 1998; Catanese et al. 1997), and later in 1998 June during smaller amplitude flares at both wavelengths (Sambruna et al. 2000).

4. DISCUSSION AND CONCLUSIONS

In this work we have studied the recent and historical radio and optical activity of AO 0235+164 in terms of cross-correlation, periodicity search of the radio data, spectral variability analysis, and by constructing multifrequency energy distributions.

The 1997–1998 outburst achieved the highest optical fluxes in 1997 December and a secondary maximum in 1998 August. The 1997 December optical flare did not show a simultaneous radio counterpart, and the decline after 1998 August was much faster in the optical band.

In order to obtain information about possible correlations between radio and visible bands, we have utilized a variety of cross-correlation techniques. The best results were obtained for the ZDCF method. We found a lag of 103^{+93}_{-19} days between the B band and 8.0 GHz light curves, but the cross-correlation coefficient is small ($r = 0.49$). The correlation between the other optical and radio bands did not yield a significant result because of the undersampling in the data sets. We also found a lag of 134^{+15}_{-113} days between the 14.5 and 4.8 GHz light curves. The cross-correlation coefficient is also small ($r = 0.62$). We have performed a periodicity search in the radio light curves, motivated by the fact that the prominent radio flares appear in regular time intervals (Fig. 2). We found a highly significant peak in the periodogram at a frequency which corresponds to a timescale of 5.8 yr.

We have analyzed information on the optical spectral variability of the source. We find that the slope of the spectrum is variable, and that the mean $B-V$ slope is different from the mean $R-I$ slope (here we have to emphasize that the results on the spectral slope are sensitive to the amount of absorption assumed). Moreover, from the $B-V$ and $R-I$ slopes plot, we found that the source can be in two different spectral states: in the first, there is a single power law with variable slope, but the slope values do not correspond to the source flux state. In the second phase, the $R-I$ spectrum has a slope of ~ -1.3 but the $B-V$ spectrum can have any slope in the range $-1 < a_{BV} < 1.5$.

Finally, we have constructed multiwavelength spectral energy distributions during and before the 1997 December outburst. We find the usual double-hump structure characteristic of blazars, with evidence that the first (synchrotron) peak shifted to higher than infrared/optical frequencies during the outburst. This behavior is similar to Mrk 501.

In what follows we will discuss our results in terms of the standard model for the nonthermal emission from blazars (Blandford & Königl 1979). According to this model, a well-collimated jet of magnetized and relativistic plasma with Lorentz factor γ flows out of the nucleus near the speed of light. The produced synchrotron radiation in the ambient magnetic field is beamed in the forward direction into a cone of opening angle $1/\gamma$.

4.1. *The Radio Periodicity*

To our knowledge, AO 0235 is the first BL Lac object that shows strong evidence for periodicity in the radio band. No such evidence has been found in the radio light curves of other BL Lac objects (Aller et al. 1999). The source sample of Aller et al. (1999) included AO 0235 as well. The main difference between theirs and the present work is that we use a longer data set for AO 0235 which includes the 1997/1998 outburst. The appearance of this outburst renders the evidence for periodicity significant. Even if the predicted radio outburst of AO 0235 in late 2003 materializes, thus confirming the existence of periodic radio-flux variations in this object, we cannot be certain that AO 0235 is unique among other BL Lac objects in this respect. Longer, better sampled radio light curves may show evidence for periodicity in the light curves of other objects as well.

The only other object that exhibits periodicity in its (optical) flux variations is OJ 287 (Sillanpää et al. 1996). In this object it is not clear that the periodicity is present at the radio wavelengths as well (e.g., Pietilä et al. 1999). However, there appears to be a connection between optical and radio flares in OJ 287 since the second of the periodic optical flares is simultaneous with radio flares (Valtaoja et al. 2000). As we have already mentioned in § 3.2, all the major, periodic radio flares of AO 0235 have optical counterparts. Consequently, despite the fact that the optical data do not show the periodicity in the periodogram analysis, there is probably a connection between the periodic radio flares and optical flares. Well sampled optical and radio light curves (mainly during the predicted future outburst) will allow a better comparison between the optical/radio flares in AO 0235 and those in OJ 287.

One possible explanation for the periodic appearance of the radio flares is that they reflect a real, periodic increase in the intrinsic magnetic field strength of the jet in AO 0235. The jets in blazars are accelerated either at the unipolar generator formed around a black hole threaded by an accretion-deposited magnetic field (Blandford & Znajek 1977) or in a magnetized accretion disk that is differentially rotating around the black hole (Lovelace 1976; Blandford & Payne 1982). Another possibility is that the magnetic field in the disk is generated via a gravitomagnetic dynamo (Khanna & Camenzind 1995). The observed periodicity that we found of 5.8 yr may ultimately be connected to such a periodic dynamo. In other words, it is possible that the situation may be akin to the dynamo generation of magnetic fields at the differentially rotating and convective stellar interiors where cyclic variations in the magnetically sensitive H and K lines of singly ionized calcium have been observed in about 30% of 111 stars monitored in the last decades (Baliunas et al. 1995, 1996). In this case, periods from a few years to longer than the solar magnetic cycle of about 11 years have been observed. Whatever the acceleration mechanism of the electrons in the jet, periodic changes in the magnetic field strength can cause the periodic formation of shock waves propagating along the jet. Those shocks could be responsible for the major flares in the radio light curves (Ghisellini et al. 1985) and, hence, introduce the observed periodicity.

Alternatively, the 5.8 yr variability timescale could have a Keplerian origin. A magnetized spot on the surface of the accretion disk around the supermassive object could be responsible for the observed variability, if this region involves a local strengthening of the B field, which varies on a timescale equal to the local Keplerian timescale. In this case, electrons would be radiating in the enhanced field via synchrotron radiation. If we assume that the accreting object in AO 0235 is a supermassive black hole, then a natural timescale is the Keplerian period of the innermost stable orbit in this accretion disk. Such an orbit lies at 3 Schwarzschild radii for a nonrotating black hole. The period of the innermost stable orbit depends only on the black hole mass and spin. In this way there is the possibility to provide some estimate of the mass and spin of the central black hole from a fixed high-frequency feature in the power spectrum. The period of the innermost stable orbit is $T = 14.4 M_9$ yr for a Schwarzschild black hole of mass $M_{\rm BH}$, with $M_9 = M_{\rm BH}/10^9\ M_\odot$ (Shapiro & Teukolsky 1983). Then, if the observed 5.8 yr periodicity is related to such a feature, the implied black hole mass is $4 \times 10^8\ M_\odot$, a value appropriate for blazars (Becker & Kafatos 1995). Note that oscillations in black hole accretion disks as a result of relativistic effects near the Schwarzschild radius have also been developed, and the period of such oscillations depends pri-

marily on the mass and spin of the central black hole, leading also to a similar estimate of the black hole mass, if it is not rotating (Nowak et al. 1997).

It is intriguing that the situation may be analogous to the case of quasi-periodic oscillations (QPOs) observed in the microquasar GRS 1915+105 where the radio, infrared, and X-ray intensities change drastically on a variety of timescales from subseconds to days. For example, a dominant feature in X-rays varying with a constant centroid frequency of 67 Hz has been used in order to estimate with the above argument that the black hole mass is about 33 $M_{\odot}$ (Greiner et al. 1996; Morgan et al. 1997; Eikenberry et al. 1998). In this case the microquasar exhibits quasi-regular X-ray/IR/radio flares suggesting the disappearance and followup replenishment of the inner accretion disk seen in X-rays and the ejection of relativistic plasma clouds observed as synchrotron emission first at infrared and later at radio wavelengths (Mirabel & Rodriguez 1999).

4.2. *The Optical/Radio Cross-Correlation*

The accumulation of a larger number of optical and radio data over the period of the last 20–25 years has allowed us to investigate the optical/radio correlated flux variations in the historical light curves of a large number of quasars and BL Lac objects (Tornikoski et al. 1994; Clements et al. 1995). Using the DCF method, these authors found significant optical/radio correlated variations with time delays less than $\sim$33 yr and $\sim$1.5 yr, respectively, in many of the studied objects. In all cases the optical variations lead those seen in the radio. The main reason for not finding significant correlations in the other objects was the lack of well-sampled radio and optical light curves. Perhaps, if the sampling of the light curves improves in the future, optical/radio correlated variations will be established in the majority of radio-loud AGNs. Therefore, our result of significant optical/radio correlations in AO 0235 implies that, in this respect, this source is rather a typical than a special case among other BL Lac objects. Furthermore, our correlation analysis results are in agreement with those of previous studies for this source.

Stevens et al. (1994) using high-frequency radio data (from 375 to 22 GHz) found no delays between the variations in the 375–150 GHz light curves, and a 20 ± 40 day delay between the 37 and 22 GHz light curves. Our and past results are in agreement with models that involve shocks propagating along a relativistic jet whose particle density and magnetic field decrease outward (Marscher & Gear 1985). According to the model, flares start at the optical-infrared frequencies and evolve in three stages: Compton, synchrotron, and adiabatic. In the first two stages, the flare evolution can be understood in terms of radiative losses, while in the last stage the flare evolution can be understood in terms of evolution of the emitting region. The lag between the 14.5 and 4.8 GHz data that we found, and the possible lag between the 37 and 22 GHz that Stevens et al. (1994) found, indicate that at frequencies less than 37 GHz flares have reached the adiabatic expansion stage. In this stage the flare peak is expected to move from higher to lower frequencies and the lag between different band light curves corresponds to the time taken for the frequency turnover to evolve from one frequency band to the other. A strong indication that the flares, at least below 14.5 GHz, have reached the adiabatic expansion stage is provided by the fact that the normalized variability amplitude decreases from the 14.5 to 4.8 GHz light curves. This is expected, since in this stage the peak flux (i.e., the flux amplitude) decreases with frequency. Furthermore, the longer decay timescales at lower frequencies can also explain the fact that the 4.8 GHz light curve looks "smoother" than the 14.5 GHz (Fig. 2) and, hence, the rather weak correlation between the two light curves, i.e., the fact that $r < 1$.

Our optical/radio cross-correlation results show a correlation between the B and 8 GHz light curves with a lag of $\sim$3 months, in the sense that optical variations lead those in the radio band. Clements et al. (1995), using a subset of our data set and the DCF technique, found a weak ($r \sim 0.3$) correlation at lag $\sim$2 months between the B band and the 8 GHz light curves. The fact that using an improved cross-correlation technique and a larger data set we also detect a correlation (stronger than previously) at a similar lag forces us to consider the possibility that this correlation is due to the fact that the particles radiating in the optical and radio wavelengths are physically related.

Such a relation is expected in the model of the propagating shock assuming that the optical outbursts correspond to the initial stage of the flares seen in the radio band. In this case, the optical/radio lag of $\sim$3 months corresponds to the time taken for the outbursts to evolve from the initial stage to the adiabatic expansion stage. Furthermore, the flare evolution timescales (rise/decay) in the optical regime are much shorter, since they are dominated by radiative losses rather than the evolution of the emitting region. As a result, when compared to the radio the optical light curves are expected to look much more erratic (as is the case; see Figs. 1 and 2) and r to have a value less than 1.

However, if there is a physical connection between the two bands, why are there some optical flares with no radio counterparts (like, for example, flare "op2" in Fig. 1)? One possibility is that the shock is radiative, in which case it dissipates rapidly and is unable to evolve appreciably down the jet (Marscher & Gear 1985). In this case, the slope of the optically thin synchrotron emission is less than -0.5. During the "op2" flare, we have three simultaneous B and V measurements (MJD 43,903.5, 43,906.5, and 43,907.5). The respective α_{BV} values are -0.11 ± 0.29, -0.15 ± 0.37, and 0.64 ± 0.27. The mean value is 0.19 ± 0.17, well above the limit when the shock becomes radiative, assuming that the B and V bands are in the optically thin region of the spectrum.

Stevens et al. (1994) claim that for most of the objects in their sample the early phase of the flares happens at frequencies between 375 and 150 GHz based on the lack of detectable lags between the light curves at these frequencies. However, the sampling of the AO 0235+164 light curves in these frequencies is not good. In fact, Figure 1 in Stevens et al. (1994) shows that the 375, 270, 230, and 150 GHz light curves have similar amplitude, while the K-band light curve has a much larger amplitude, similar to the amplitude of our optical light curves. This situation is consistent with the assumption that between 375 and 150 GHz the flares in AO 0235+164 are in the synchrotron stage of their development (where the flare amplitudes are expected to be constant). Therefore, the initial Compton-loss stage should appear at higher frequencies (i.e., infrared-optical).

Another possibility is that the optical flares without a radio counterpart could be caused by gravitational microlensing. Abraham et al. (1993) discuss extensively the possibility that AO 0235+164 is being strongly microlensed by

individual stars in the foreground galaxy. They dismiss this possibility as unlikely, based on the fact that microlensing can result in amplifications of small amplitude, in contrast to the large amplitude/short timescale variability observed for this object. Saust (1992) reached the same conclusion based on the fact that the emission-line variability in AO 0235+164 is much larger than what is expected from microlensing. The effects on light curves due to microlensing when there are many stars in the beam of a lensed object are complex and difficult to estimate, unless one uses Monte Carlo simulations. This is beyond the scope of the present work; however, we briefly consider the effects induced on the optical light curves by the passing of an isolated microlens in front of the optical source in AO 0235+164. Recently, Kraus et al. (1999) suggested that a peculiar radio variability event in 1992 could be caused by gravitational microlensing by a solar mass–like object situated at $z = 0.525$. During the "op2" flare (which does not show a radio counterpart) the B flux of AO 0235+164 increased by a factor of ~ 20 in ~ 30 days. If this event was caused by microlensing by a solar mass object, for a magnification of ~ 20 the size of the optical source should be ~ 10 times smaller than the radio source size in AO 0235+164 (eq. [19] in Krauss et al. 1999). As these authors comment, the small intrinsic radio source size suggested by the gravitational lensing scenario implies a Doppler factor value which is very high (~ 100). A smaller optical source would imply an ever larger Doppler factor value, substantially higher than the canonical value of ~ 10 (e.g., Ghisellini et al. 1993). Although microlensing may affect the optical/radio light curves of AO 0235+164, it is probably not the dominant effect in defining the variability properties in this object.

4.3. *Optical Spectral Variability and the Peak Synchrotron Frequency*

As mentioned in § 3.3, the peak synchrotron component in the SED is usually located at IR/optical wavelengths. Although the data coverage was limited, the 1997 December SED of the object shows that the synchrotron peak is most probably located above the B band. If we approximate the local emission in the jet as a homogeneous source emitting synchrotron radiation, the synchrotron peak frequency $\nu_{\rm peak} \propto B\gamma^2_{\rm peak}$, where B is the magnetic field and $\gamma_{\rm peak}$ is the electron energy determined by the competition between acceleration and cooling (Pian et al. 1998; Sambruna et al. 1996). Different synchrotron peak frequencies can naively be interpreted as due to different increase of the electron energies and/or the source magnetic field (as compared to the values of the quiescent state) due to plasma compression through the shock. Consequently, shocks with variable strength and/or at different locations in the jet will produce flares with different initial turnover frequencies in the optical/infrared regime.

Flares with peak synchrotron frequencies above the optical band should produce flux-related spectral variations in the optical band due to the flare evolution. This correlation can be diluted if flares with different peak synchrotron frequencies are present at the same time in the light curves. This situation can justify the apparently chaotic optical spectral variability that the source exhibits (Fig. 9). On the other hand, reacceleration of the electron population could also explain the complex spectral behavior. In Figure 10 we observe that when α_{RI} is ~ -1.5 (which corresponds to the steepest slope), α_{BV} can have a value anywhere between -1.5 and 1. The different α_{BV} values could be the result of local reacceleration of the decaying electron population due to inhomogeneities caused by jet turbulence. This reacceleration could happen at all times, but only when the main flare spectrum is sufficiently steep can we observe its effects (i.e., the flattening of the $B-V$ slope). In fact, when one considers only these cases when the whole optical spectrum is well fitted by a single power law, the slope is correlated with the source flux: the spectrum becomes harder as the source flux increases. Regular B to I monitoring of the source is needed to investigate further if reacceleration operates. In this case, we should be able to observe the I-band variations leading those in the other optical bands.

As we mentioned in the introduction, AO 0235+164 is one of the most complex blazars. Its nature remains controversial. Multifrequency observations, with regular, dense sampling patterns, at as many bands as possible are required in order to decide whether the "standard model" (i.e., shocks propagating down an inhomogeneous model) can explain the variability behavior of this source. The variability amplitude values, the cross-correlation results, even the spectral variability behavior of the source are in agreement with such a model, but many details are still missing. We suggest that, apart from the regular monitoring data, high-resolution spatial observations are needed to be brought in, perhaps combining VLBI, *HST*, *Chandra* observations, that would be triggered if optical and/or radio monitoring indicated an outburst was in progress. Densely sampled light curves at γ-rays, coordinated with ground-based optical observations, are also necessary to follow the energy dependence of the flare and gain more detailed insights into the structure and energetics of the jet.

We wish to thank Aimo Silanpää and his group for access to some of their unpublished data and also the data compilation out of their continuing campaign of long-time monitoring at Tuorla Observatory, Pikkio, Finland. This research has made use of data from the University of Michigan Radio Astronomy Observatory (UMRAO), which is supported by the National Science Foundation and by funds from the University of Michigan. Data have been collected also from the NASA/IPAC Extragalactic Database (NED), which is operated by the Jet Propulsion Laboratory, California Institute of Technology, under contract with the National Aeronautics and Space Administration. Skinakas Observatory is a collaborative project of the University of Crete, the Foundation for Research and Technology-Hellas, Greece, and the Max-Planck-Institut für extraterrestrische Physik, Munich, Germany. One of us (M. Roy) is deeply indebted to the Center for Earth Observing and Space Research, George Mason University, for support during 1999 and for providing the computation facilities during 1999.

REFERENCES

Abraham, R. G., Crawford, C. S., Merrifield, M. R., Hutchings, J. B., & McHardy, I. M. 1993, ApJ, 415, 101
Alexander, T, 1997, in Astronomical Time ser., ed. D. Maoz, A. Sternberg, & E. M. Leibowwitz (Dordrecht: Kluwer), 163 (available online at http:// www.sns.ias.edu/tal/zdcf2.html)
Aller, M. F., Aller, H. D., Hughes, P. A., & Latimer, G. E. 1999, ApJ, 512, 601
Angel, J. R. P., & Stockman, H. S. 1980, ARA&A, 18, 321
Bååth, L. B. 1984, in IAU Symp. 110, VLBI and Compact Radio Sources, ed. R. Fanti, K. Kellermann, & G. Setti (Dordrecht: Reidel), 127
Baliunas, S. L., et al. 1995, ApJ, 438, 269
Baliunas, S. L., Nesme-Ribes, E., Sokoloff, D., & Soon, W. H. 1996, ApJ, 460, 848
Balonek, T. J., & Dent, W. A. 1980, ApJ, 240, L3
Becker, P. A., & Kafatos, M. 1995, ApJ, 453, 83
Bevington, P. R. 1969, Data Reduction and Error Analysis for the Physical Sciences (New York: McGraw-Hill)
Blandford, R. D., & Königl, A. 1979, ApJ, 232, 34
Blandford, R. D., & Payne, D. G. 1982, MNRAS, 199, 883
Blandford, R. D., & Znajek, R. 1977, MNRAS, 179, 433
Brown, L. M. J., et al. 1989, ApJ, 340, 129
Burbidge, E. M., Beaver, E. A., Cohen, R. D., Junkkarinen, V. T., & Lyons, R. W. 1996, AJ, 112, 2533
Burbidge, G., & Hewitt, A. 1992, in Variability of Blazars, ed. E. Valtaoja & M. Valtonen (Cambridge: Cambridge Univ. Press), 415
Cardelli, J. A., Clayton, G. C., & Mathis, J. S. 1989, ApJ, 345, 245
Catanese, M., et al. 1997, ApJ, 487, L143
Chu, H. S., Bååth, L. B., Rantakyrö, F. T., Zhang, H. S., Nicholson, G. 1996, A&A, 307, 15
Clements, S. D., Smith, A. G., Aller, H. D., & Aller, M. F. 1995, AJ, 110, 529
Cohen, R. D., Smith, H. E., Junkkarinen, V. T., & Burbidge, E. M. 1987, ApJ, 318, 577
Edelson, R. A., & Krolik, J. H. 1988, ApJ, 333, 646
Edelson, R. A., et al. 1996, ApJ, 470, 364
Eikenberry, S, Matthews, K., Morgan, E., Remillard, R., & Nelson, R. 1998, ApJ, 494, 61
Fossati, G., Maraschi, L., Celotti, A., Comastri, A., & Ghisellini, G. 1998, MNRAS, 299, 433
Gabuzda, D. C., & Cawthorne, T. V. 1996, MNRAS, 283, 759
Gaskell, C. M., & Peterson, B. M. 1987, ApJS, 65, 1
Ghisellini G., Maraschi, L., & Treves, A. 1985, A&A, 146, 204
Giommi, P., Ansari, S. G., & Micol, A. 1995, A&AS, 109, 267
Giommi, P., Barr, P., Garilli, B., Maccagni, D., & Pollock, A. M. T. 1990, ApJ, 356, 432
Giveon, U., et al. 1999, MNRAS, 306, 637
Greiner, J., Morgan, E. H., & Remillard, R. 1996, ApJ, 473, L107
Hartman, R. C., et al. 1999, ApJS, 123, 79
Hewitt, A., & Burbidge, G. 1993, ApJS, 87, 451
Impey, C. D. 1987, in Superluminal Radio Sources, ed. J. A. Zensus & T. J. Pearson (Cambridge: Cambridge Univ.Press), 231
Jones, D. L., Unwin, S. C., Bååth, L. B., Davis, M. M. 1984, ApJ, 284, 60
Khanna, R., & Camenzind, M. 1996, Astron. Lett. Commun., 34(1–6), 53
Kraus, A., et al. 1999, A&A, 344, 807
Ledden, I. E., Aller, H. D., & Dent, W. A. 1976, Nature, 260, 752
Leighly, K. M. 1999, ApJS, 125, 297
Lomb, N. R. 1976, Ap&SS, 39, 447
Lovelace, R. V. E. 1976, Nature, 262, 649
MacLeod, J. M., Andrew, B. H., & Harvey, G. A. 1976, Nature, 260, 751
Madejski, G., Takahashi, T., Tashiro, M., Kubo, H., Hartman, R., Kallman, T., & Sikora, M. 1996, ApJ, 459, 156
Marscher, A. P., & Gear, W. K. 1985, ApJ, 298, 114
McGimsey, B. Q., Miller, H. R., & Williamson, R. M. 1976, AJ, 81, 750
Mead, A. R. G., Ballard, K. R., Brand, P. W. J. L., Hough, G. H., Brindle, C., & Bailey, J. A. 1990, A&AS, 83, 183
Mirabel, I. F., & Rodriguez, L. F. 1999, ARA&A, 37, 409
Morgan, E. H., Remillard, R., & Greiner, J. 1997, ApJ, 482, 993
Mukherjee, R., et al. 1997, ApJ, 490, 116
Nowak, M. A., Wagoner, R. V., Begelman, M. C., & Lehr, D. E. 1997, ApJ, 477, L91
O'Dell, S. L., et al. 1988, ApJ, 326, 668
O'Dell, S. L., Puschell, J. J., Stein, W. A., & Warner, J. W. 1977, ApJ, 214, L105
Pian, E., et al. 1998, ApJ, 492, L17
Pica, A. J., Smith, A. G., & Pollock, J. T. 1980, ApJ, 236, 84
Pietilä, H., et al., 1999, A&A, 345, 760
Press, W. H., Teukolsky, S. A., Vetterling, T., & Flannery, B. P. 1992, Numerical Recipes in FORTRAN (2d ed.; Cambridge: Cambridge Univ. Press)
Quirrenbach, A., et al. 1992, A&A, 258, 279
Rieke, G. H., Grasdalen, G. L., Kinman, T. D., Hintzen, P., Wills, B. J., & Wills, D. 1976, Nature, 260, 754
Roberts, M. S., Brown R. L., Brundage W. D., Rots, A. H., Haynes, M. P., & Wolfe, A. M. 1976, AJ, 81, 293
Romero, G. E., Combi, J. A., Benaglia, P., Azcarate, I. N., Cersosimo, J. C., & Wilkes, L. M. 1997, A&A, 326, 77
Ryter, C. E. 1996, Ap&SS, 236, 285
Sambruna, R. M., Barr, P., Giommi, P., Maraschi, L., Tagliaferri, G., & Treves, A. 1994, ApJ, 434, 468
Sambruna, R. M., Maraschi L., & Urry, C. M. 1996, ApJ, 463, 444
Sambruna, R. M., et al. 2000, ApJ, 538, 127
Saust, A. B. 1992, A&A, 266, 101
Scargle, J. D. 1982, ApJ, 263, 835
Schramm, K.-J., Borgeest, U., Kühl, D., von Linde, J., Linnert, M. D., & Schramm, T. 1994, A&AS, 106, 349
Shapiro, S. L., & Teukolsky, S. A. 1983, Black Holes, White Dwarfs, and Neutron Stars (New York: Wiley)
Shen, Z.-Q., et al. 1997, AJ, 114, 1999
Sikora, M. 1994, ApJS, 90, 923
Silanpää, A., et al. 1996, A&A, 305, L17
Smith, P. S., Balonek, T. J., Elston, R., & Heckert, P. A. 1987, ApJS, 64, 459
Smith, P. S., Balonek, T. J., Heckert, P. A., Elston, R., & Schmidt, G. D. 1985, AJ, 90, 1184
Spinard, H., & Smith, H. E., 1975, ApJ, 201, 275
Stevens, J. A., Litchfield, S. J., Robson, I. E., Hughes, D. H., Gear, W. K., Teräsranta, Valtaoja, E., & Tornikoski, M. 1994, ApJ, 437, 91
Stickel, M., Padovani, P., Urry, C. M., Fried, J. W., & Kuhr, H. 1991, ApJ, 374, 431
Takalo, L. O., et al. 1998, A&AS, 129, 577
Teräsranta, H., et al. 1992, in Variability of Blazars, ed. E. Valtaoja & M. Valtonen (Cambridge: Cambridge Univ. Press), 59
Thompson, D. J., et al. 1995, ApJS, 101, 259
Tornikoski, M., Valtaoja, E., Teräsranta, H., Smith, A. G., Nair, A. D., Clements, S. D., & Leacock, R. J. 1994, A&A, 289, 673
Ulrich, M.-H., Maraschi, L., & Urry, C. M. 1997, ARA&A, 35, 445
Urry, C. M., Sambruna, R. M., Worrall, D. M., Kollgaard, R. I., Feigelson, E. D., Perlman, E. S., & Stocke, J. T. 1996, ApJ, 463, 424
Valtaoja, E., Teräsranta, H., Tornikoski, M., Silanpää, A., Aller, M. F., Aller, H. D., & Hughes, P. A. 2000, ApJ, 531, 744
von Montigny, C., et al. 1995, ApJ, 440, 525
Webb, J. R. 1992, in Variability of Blazars, ed. E. Valtaoja & M. Valtonen (Cambridge: Cambridge Univ. Press), 415
Webb, J. R., & Smith, A. G. 1989, A&A, 220, 65
Webb, J. R., Smith, A. G., Leacock, R. J., Fitzgibbons, G. L., Gombola, P. P., & Shepherd, D. W. 1988, AJ, 95, 374
Wolfe, A. M., Briggs, F. H., & Davis, M. M. 1982, ApJ, 259, 495
Yanny, B., York, D. G., & Gallagher, J. S. 1989, ApJ, 338, 735